Alwaha Sci. Publ. Services

Journal of Renewable Energy and Technology

Available at https://asps-journals.com

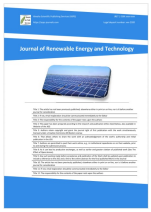

Control strategy of a standalone variable speed wind energy conversion system based on direct drive permanent magnet synchronous generator

Messaoud Mayouf ✉

Electrical engineering department, Faculty of Technology, Mohamed Boudiaf University of Msila, Algeria

Received January 1, 2022
Revised May 9, 2022
Accepted September 8, 2022
Published online: November 11, 2022

Keywords
Field-oriented control
Permanent magnet generator
PI controller
Torque estimation
Voltage regulation
Wind energy conversion system

Abstract: In this paper, we propose a control strategy for a stand-alone wind energy conversion system (WECS) based on a direct drive permanent magnet synchronous generator (PMSG), loaded on a DC-type charge. In the considered wind-power generating system, the generator provides a DC voltage to the load through a three-phase rectifier, controlled by the Pulse Width Modulation (PWM) technique. The main control strategy target is to maintain the DC voltage insensitive to fast changes in wind speed and load, by offsetting the generator output current with the charge current. The approach adopted in this paper is based on the estimate of the PMSG electromagnetic torque assuming that wind velocity remains quasi-stationary in a steady state. The instant power reference is assessed by the charge controller according to the rated DC bus voltage, using actual electrical measurements as the voltage and current. To achieve adequately the power decoupling, the field-oriented control is used with conventional PI-type regulators to provide direct and quadrature control reference voltages and ensure DC bus voltage regulation. To assess the proposed control strategy efficiency, the simulation model was subjected to different load and wind speed variations. Simulation results performed using the MATLAB Simulink model show high accuracy and strength during steady-state and transient operations.

1. Introduction

Most wind farms are based on grid-connected production systems. This is accompanied by technical constraints and high costs associated either with the extension of electrical systems or the use of self-contained energy sources such as the use of diesel generators. Renewable energy technologies are capable of generating electric power directly at sites provided by low-power, high-design wind power generators, like direct drive permanent magnet synchronous generators.

This context leads to the simplification and development of wind system structures that are controlled to the maximum extent by the use of electronic cutting techniques. The main desired targets of such studies are the extending of exploitable wind velocities while optimizing these performances at a lower cost.

Several configurations have been proposed by researchers, dedicated to low-energy wind systems, and designed to charge batteries. In (Aissou et al. 2016) a nonlinear predictive control is implemented with a stand-alone wind system based on a direct drive permanent magnet synchronous generator (PMSG), to adjust the battery voltage used downstream of a pulse with a modulation (PWM) rectifier. The wind power structures proposed by (Pannell et al, 2013; Lee et al, 2018) used a damp resistor controller to dispel excess power throughout fault or over-generation based on the chopper control to

✉ Corresponding author. E-mail address: messaoud.mayouf@univ-msila.dz

maintain the battery voltage. The variable speed PMSG based wind energy conversion system proposed by (Minh et al, 2012) used two fuzzy controllers to optimize the operation of both the wind turbine and the battery voltage according to wind speed and load demand. In (Agrebi et al, 2021), a three-blade turbine driving directly three phases PMSG is implemented using a transformer combined with a diode rectifier delivering on a DC bus linking. This configuration requires the connection of a generator downstream transformer to increase the turbine energy efficiency, regardless of battery voltage changes. Moreover, it revealed correlativity between the wind turbine recovered power and the DC bus voltage. With judicious natural adaptation of the impedance to the source variations, this simple passive structure could get better in the field of standalone wind systems. The structure proposed by (Shi and Li, 2004) includes a small vertical wind turbine. It supplies a variable load according to a well-defined consumption profile which is managed by an electronic interface. In this structure, the MPPT algorithm uses the principle of artificial neural networks. The experimental results of this study show its energy limit without maximizing control by adapting the grid impedance to the wind speed. The algorithm control used by (Abdulelah et al, 2021) is based on direct power control (DPC) with an AC/DC converter system with a PI controller for the DC link voltage. In the Standalone PMSG based wind-generating system studied by (Elmorshedy et al, 2021), the speed is estimated based on the model reference adaptive system (MRAS) to adjust the DC-link voltage under different circumstances. In (Benlahbib et al, 2019), a Fractional order PID controller is used for DC link voltage control in a standalone PMSG hybrid system including wind turbine and battery packs. In the grid-connected wind power system presented by (Zhou et al, 2020), a second-order linear active disturbance rejection control (LADRC) is used in the voltage outer loop to suppress the wide range fluctuation of the DC voltage under disturbances.

In this paper, a simple structure of a stand-alone wind system delivering on a DC bus through a PWM rectifier, using conventional PI controllers is suggested. The strategy proposed in this paper is based on the estimate of the PMSG electromagnetic torque. Assuming that wind speed varies slowly in a steady state, the result is that the rotation speed also keeps an almost constant quantification.

2. WECS modelling

The system under study is shown in Figure 1. It consists of a direct-drive PMSG wind turbine. The generator is cascaded with a three phases PWM rectifier. In this diagram, R represents the charge resistance, v_{dc} is the DC bus voltage, I_{dc} is the rectifier output current, while I_R is the charge input current.

The battery charger provides power to the battery while ensuring continuous voltage control. A supervision system generates the reference signals to the system to control the PWM-controlled rectifier by modifying instantly the corresponding duty cycles.

2.1. Wind turbine modelling

The structure considered is that of a variable speed, fixed pitch, rigid drive train WECS mechanical torque developed by the rotor T_m, and the tip-speed ratio λ, are given by:

$$T_m = \frac{\rho \pi R_t^2 c_p(\lambda,\beta) v^3}{2 w_t} \quad (1)$$

$$\lambda = \frac{w_t R_t}{v} \quad (2)$$

T_m is dependent on the air density ρ, the blade length of the turbine R_t, the wind speed v, the low shaft speed ω_t, and the power coefficient c_p, which denotes the percentage of power extracted from the available power in the wind. The power coefficient can be approximated based on the tip-ratio and the pitch angle β as (Hostettler and Wang, 2015):

$$C_p(\lambda,\beta) = c_1\left(\frac{c_2}{\lambda_i} - c_3\beta - c_4\right)\exp\left(-\frac{c_5}{\lambda_i}\right) \quad (3)$$

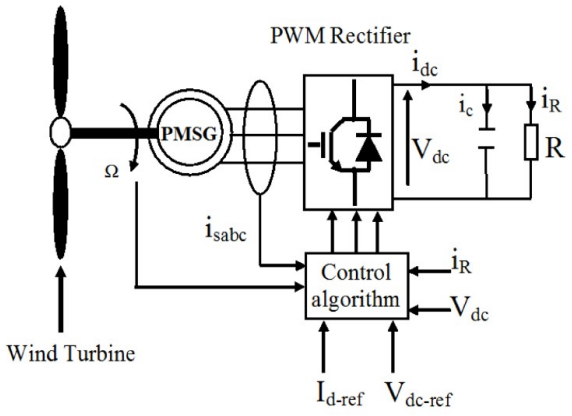

Fig. 1 Studied system diagram.

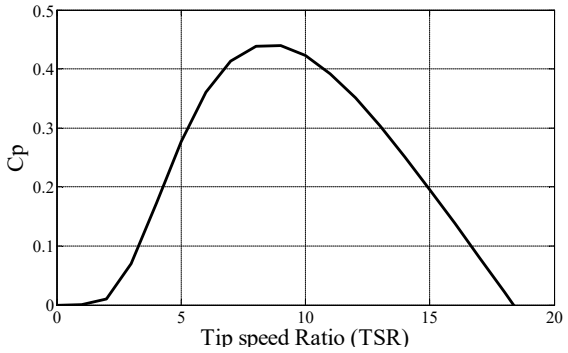

Fig. 2 Power coefficient vs Tip Speed Ratio.

Where;

$$\lambda_i = \left(\frac{1}{\lambda + \beta c_6} - \frac{c_7}{\beta^3 + 1}\right)^{-1} \quad (4)$$

Figure 2 shows the power coefficient curve of the studied turbine, where C_1=0.39, C_2=116, C_3=0.4, C_4=5, C_5=16.5, C_6=0.089, C_7=0.035, and β=2°

2.2. PMSG mathematical model

Using the (d-q) synchronous reference frame, PMSG electrical equations are given by (Mayouf and bakhti, 2018):

$$V_d = -R_s I_d - L_d \frac{d}{dt} I_d + \omega L_q I_q \quad (5)$$

$$V_q = -R_s I_q - L_q \frac{d}{dt} I_q - \omega L_d I_d + \omega \psi_f \quad (6)$$

In Eqs. (5) and (6), V_d and V_q represent d-q axis statoric voltages, L_d and L_q are inductance values in d-q axis reference, R_S is the statoric resistance by phase, I_d and I_q represent direct and quadrature axis currents, while Ψ_f is the permanent magnet flux. PMSG electromagnetic torque is given by:

$$T_{em} = \frac{3}{2} P[(L_q - L_d) i_d i_q + i_q \psi_f] \quad (7)$$

P: represents PMSG Number of pole pairs.

Wind system dynamics are given by:

$$T_m - T_{em} - f\Omega = J \frac{d\Omega}{dt} \quad (8)$$

In Eq. (8), T_m represents the turbine shaft torque (Nm), T_{em} is the generator electromagnetic torque (Nm), f is the viscous friction coefficient, fΩ represents the frictional torque, Ω is the rotor mechanical speed (rad/s). While J is the moment of inertia returned to the generator shaft (Kg.m^2). Direct drive PMSG synchronization peed ω and wind turbine mechanical speed Ω are linked by the relation:

$$\omega = P\Omega \quad (9)$$

2.3. PWM rectifier model

The Wind systems are characterized by extreme variations between the power electronics dynamic and mechanical dynamics. To overcome this problem, continuous models are more suitable. According to this approval, rectifier devices are considered as a set of switches that perform instant switching in response to control signals. For each switch, we define a "connection" function. It sets the switching array such as:

Sic=1 in the on case.

Sic=0 in the off case

Where index c corresponds to the switching cell and index i refers to the cell switching setting. For a three-phase converter, we define the following conversion functions $\overline{m}$:

$$\overline{m} = \begin{bmatrix} m_1 & m_2 \end{bmatrix} = \begin{bmatrix} 1 & 0 & -1 \\ 0 & 1 & -1 \end{bmatrix} \begin{bmatrix} S_{11} \\ S_{12} \\ S_{13} \end{bmatrix} \quad (10)$$

The conduction state of the converter components can be represented by a connection matrix composed of three commutation cells. Switches in control of the same cell are complementary; ie, $\forall i \in \{1,2,3\}$:

$$S_{i1} + S_{i2} = 1 \quad (11)$$

Rectifier modelling consists of expressing compound voltages based on DC bus voltage and switches states. Modulated voltages are carried out from the continuous bus voltage and connection relations as in the following expressions:

$$\begin{aligned} u_{m13} &= m_1 . V_{DC} \\ u_{m23} &= m_2 . V_{DC} \end{aligned} \quad (12)$$

Modulated single voltages are derived from modulated compound voltages according to Eq. (13):

$$\begin{cases} v_{m-1} = \frac{2}{3} . u_{m13} - \frac{1}{3} . u_{m23} \\ v_{m-2} = -\frac{1}{3} . u_{m13} + \frac{2}{3} . u_{m23} \end{cases} \quad (13)$$

Knowing that simple voltages (V_d, V_q) modulated in d-q axis reference are related to control voltages u_{dw-reg} and u_{qw-reg} by the relationships (Mayouf and Bakhti, 2021):

$$V_d = u_{dw-reg}.\frac{V_{DC}}{2} \quad (14)$$

$$V_q = u_{qw-reg}.\frac{V_{DC}}{2} \quad (15)$$

u_{dw-reg} and u_{qw-reg} are direct and quadrature converter adjustment voltages.

Simple modulated voltages are given by:

$$\begin{pmatrix} V_{s1} \\ V_{s2} \end{pmatrix} = P[(\theta)]^{-1}.\begin{pmatrix} V_d \\ V_q \end{pmatrix} \quad (16)$$

$P[(\theta)]^{-1}$ is Park transposed matrix.

The converter modulated current is given by Mayouf and Bakhti (2021):

$$i_{dc} = \frac{1}{2}.(u_{dw-reg}.I_d + u_{qw-reg}.I_q) \quad (17)$$

I_q and I_d are the quadratures and direct components of input rectifier currents.

$$\begin{pmatrix} I_d \\ I_q \end{pmatrix} = P[(\psi)].\begin{pmatrix} i_{s1} \\ i_{s2} \end{pmatrix} \quad (18)$$

3. PMSG control strategy

The strategy proposed in this paper is predicated on the estimate of the PMSG electromagnetic torque. Assuming that wind speed fluctuates slowly in a steady state, the result is that the rotation speed also keeps an almost constant quantification in a steady state. One can therefore assume that the shaft total mechanical torque is null:

$$T_{mec} = \frac{d\Omega}{dt} = 0 \quad (19)$$

We neglect also the resistant torque friction;

$$T_f = f.\Omega \approx 0 \quad (20)$$

The turbine dynamic behavior therefore given by Eq. (21):

$$T_{mec} = T_g - T_{em} - T_f = T_g - T_{em} = 0 \quad (21)$$

T_g: Turbine torque referred to the generator shaft (Nm)

T_{em}: Generator electromagnetic torque (Nm),

From Eq. (21) we deduce that:

$$T_{em} = T_g \quad (22)$$

Neglecting mechanical and resistive losses into the power conversion chain, the power supplied by the turbine P_{Tur} is therefore equal to that consumed by the load P_{Load}:

$$P_{Tur} = T_g.\Omega = P_{Load} \quad (23)$$

Finally, we deduce from Eq. (22) and Eq. (23) that PMSG electromagnetic reference torque can be estimated by:

$$T_{em} = \frac{P_{Load}}{\Omega} \quad (24)$$

From the reference DC voltage, and since all the active energy from the rectifier is consumed by the resistive part of the load, the current I_c has only the active component. It is therefore possible to consider the load power as a reference active power:

$$P_{ref} = V_{dc}.i_{dc} = V_{dc}.i_R = \frac{V_{dc}^2}{R} \quad (25)$$

The control of the DC bus voltage can therefore be carried out by using an electromagnetic torque setting. The vector control applied to the generator imposes a zero direct current reference, which will allow us from Eq. (7) to express the electromagnetic torque by:

$$T_{em} = \frac{3}{2}P.\psi_f I_{sq} \quad (26)$$

The q axis reference current is then given by;

$$I_{qref} = \frac{2}{3.p.\psi_f}T_{em-ref} \quad (27)$$

DC bus voltage can be regulated by controlling the quadrature axis current I_q. The use of conventional PI regulators in the control structure is considered. Using Eqs. (5) and (6), PPMSG mathematical model can be reformulated as follows:

$$\begin{cases} V_{sd}(p) = R_s.I_{sd}(p) + P.L_s.I_{sd}(p) - \omega.\psi_{sq}(p) \\ V_{sq}(p) = R_s.I_{sq}(p) + P.L_s.I_{sq}(p) + \omega.\psi_{sd}(p) \end{cases} \quad (28)$$

In Eq. (28), P represents the Laplace operator while the coupling terms $E_{dq}=\omega.\Psi_{dq}$ are taken as measurable disturbances, that which results in the following transfer functions:

$$G_s(p) = \frac{I_{d,q}(p)}{V_{d,q}(p) + E_{d,q}(p)} = \frac{1}{R_s}.\frac{1}{1 + T_e.p} \quad (29)$$

In Eq. (29), the electric time constant T_e is given by Eq. (30);

$$T_e = \frac{L_s}{R_s} \quad (30)$$

The I_d current control loops with PI (k_{cp}, k_{ci}) regulator are then presented in the form of the block diagram given in Figure 3.

The open loop transfer function is given by Eq. (31):

$$G_0(p) = \frac{k_{ci}}{p}\left(1+\frac{k_{cp}}{k_{ci}}.p\right).\frac{1}{R_s}.\frac{1}{1+T_e.p} \quad (31)$$

Regulator parameters are determined by the open loop compensation method, thus, the time constants are given by Eq. (32):

$$T_0 = T_e = \frac{k_{cp}}{k_{ci}} \quad (32)$$

The closed-loop transfer function becomes:

$$G(p) = \frac{G_0(p)}{1+G_0(p)} = \frac{1}{1+\frac{R_s}{k_{ci}}.p} = \frac{1}{1+T_f.p} \quad (33)$$

Based on the time constant T_f, regulator coefficients (k_{cp}, k_{ci}) can therefore be calculated using Eq. (34), Eq. (35), and Eq. (36).

$$T_f = \frac{R_s}{k_{ci}} \quad (34)$$

$$k_{ci} = \frac{R_s}{T_f} \quad (35)$$

$$k_{cp} = \frac{L_s}{T_f} \quad (36)$$

Figure 4 depicts the PMSG vector control with $I_{d\text{-}q}$ currents and voltage decoupling loops.

As with direct and quadrature currents control, the DC-bus voltage control is achieved using PI regulators, through the adjustment of the current I_{dc}. For a resistive load, the ensuing equation applies:

$$i_c = i_{dc} - i_R = C\frac{dV_{DC}}{dt} - \frac{V_{DC}}{R} \quad (37)$$

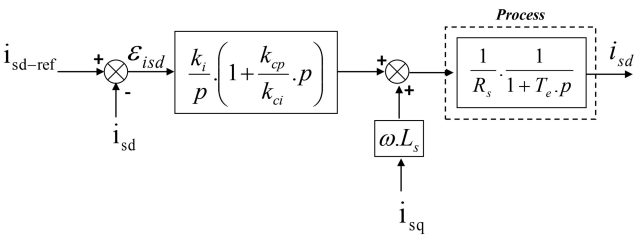

Fig. 3 I_d Current control loops.

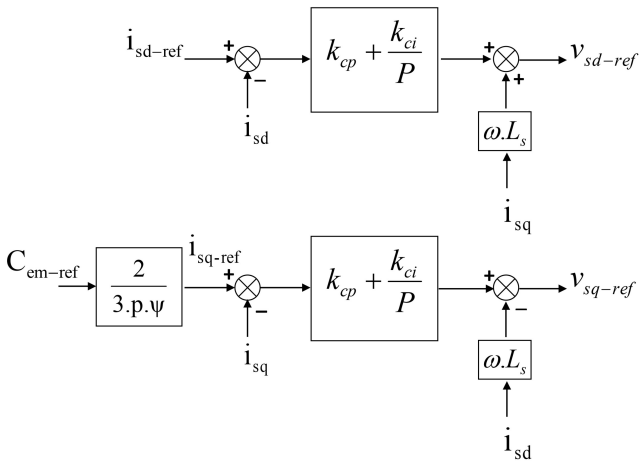

Fig. 4 PMSG field-oriented control.

4. Results and discussions

Figure 5 depicts the overall PMSG field-oriented control scheme associated with the PWM rectifier, whereas its parameters are given in Tables 1, 2, and 3. Assessing the

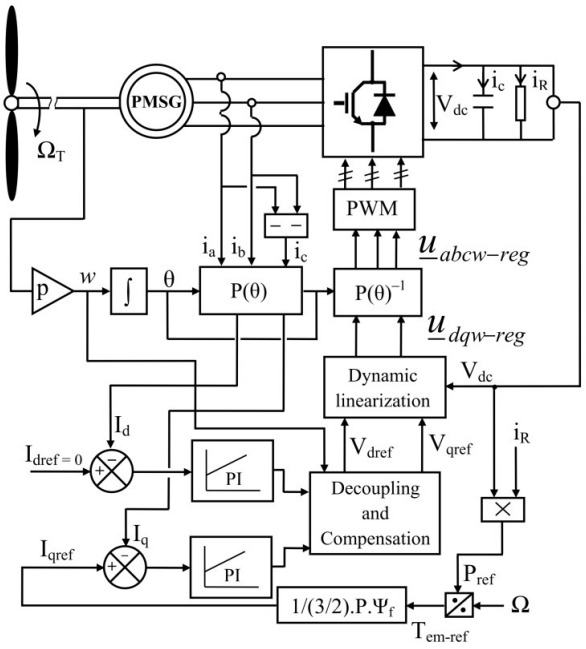

Fig. 5 Block diagram of system control.

Table 1 PMSG Parameters.

Components	Rating values
Poles number	2P=6
Resistance of stator	R_S =3.5 Ω
Magnet flux linkage	Ψf = 0.3 Wb
d-axis inductance	L_d=35 mH
q-axis inductance	L_q=35 mH
Inertia	J=0.001 Kg.m^2
Stiffness	0.001
k_{cpd}	3.5
k_{cid}	300
K_{cpq}	3.5
k_{ciq}	300

Table 2 Wind turbine parameters.

Components	Rating values
Peak Power	10 Kw
Air density	ρ=1.08 Kg.m^3
Rotor radius	R_t= 3 m

Table 3 DC bus parameters.

Components	Rating values
DC link Voltage	400 V
Capacitor	33µF

proposed strategy, the system model was subjected to fast changes in the load and the wind profile as shown in Figures 6 and 7, respectively. Figure 8 represents the constant 400 V DC- bus voltage. For a coherent load, the DC bus voltage is relatively retained unchanged throughout the wind Profile. Nevertheless, the fast load variation slightly swerves the DC voltage from the reference with overruns close to 5.5%, and therefore the component of the stator currents. The effect of load variations is more significant on the DC voltage curve. Figures 9 and 10 illustrate I_q and I_d responses, while decoupling is maintained throughout the operating regime. The main component of the DC voltage adjusting is the quadrature current I_q whose curve is perfectly similar to that of the wind profile. Direct axis current I_d is driven to zero as desired and stays there in spite of disturbances, which itself validates the flow-oriented control opted in the regulator synthesis. This proves the suitability of this technique with the proposed control approach which is based on the active power knowledge to estimate the electromagnetic torque.

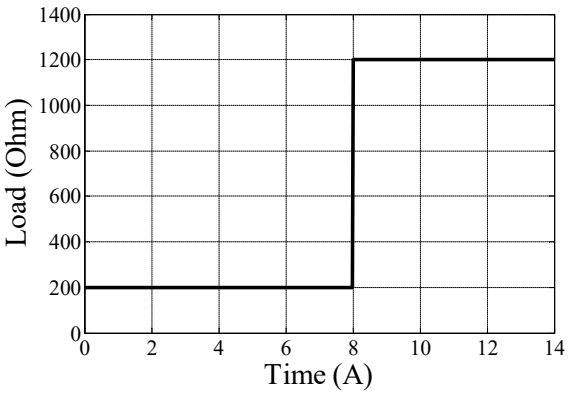

Fig. 6 Load disturbances.

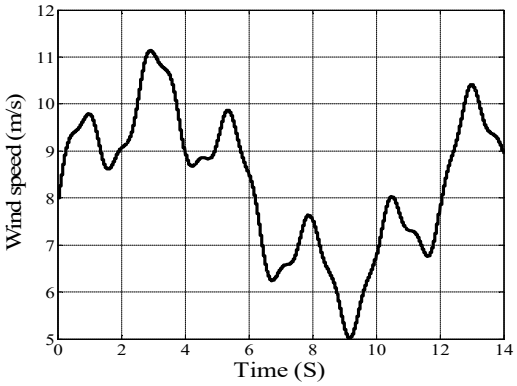

Fig. 7 Wind velocity.

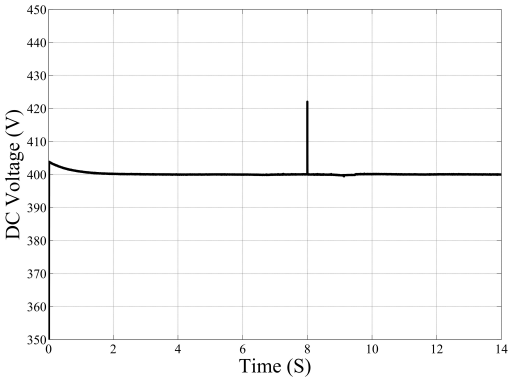

Fig. 8 DC bus voltage.

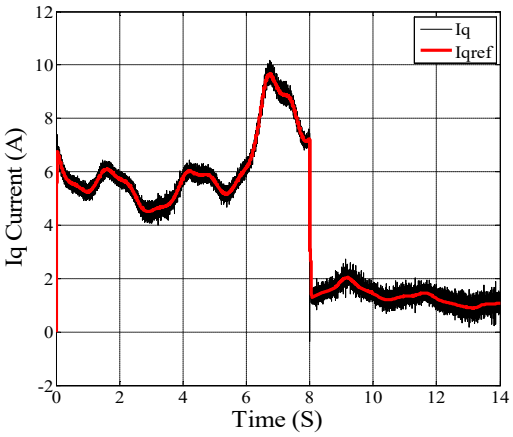

Fig. 9 I_q current.

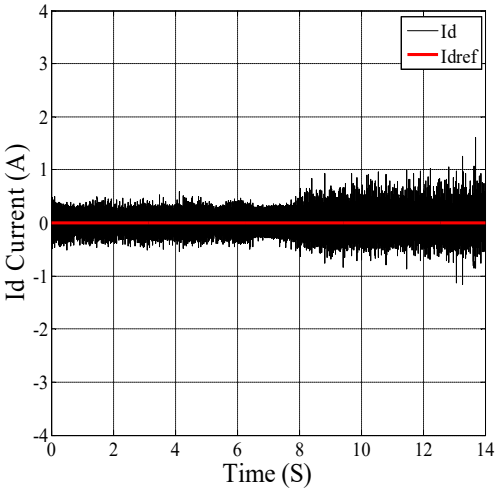

Fig. 10 I_d current.

4. Conclusion

The control strategy developed in this contribution is based on PMSG electromagnetic torque estimation in steady-state. Conventional PI regulators were applied to regulate the different electrical quantities that remained close to the reference curves, such as I_{dq} currents and battery voltage. Although the disturbances recorded in simulation results are not perfectly rectified due to speedy variations in external simulation parameters, we can positively evaluate the technique used by noticing the response speed and the robustness of the DC voltage during wind speed variations. The approach used in this work is technically simple and requires only actual measurement of the load electrical parameters without needing an exact wind speed measurement. The system is therefore designed with a reduced overall cost which supports its use in isolated sites such as irrigation, ventilation, and as emergency power in hospitals. A more secure functioning of the studied system can be achieved in the next contributions, by improving its behaviour against faults. Therefore, the useful application of the proposed approach in wind systems can be confirmed from point of view of practicality and simplicity.

Nomenclature

C	DC bus capacity, F
C_P	Dimensionless power coefficient
(d,q)	Park synchronous reference
f	Viscous friction coefficient
I_c	Capacity input current, A
I_{dc}	rectifier output current, A
I_{d-q}	d-q axis stator currents, A
I_R	Load input current, A
I_{qref}	q axis reference current, A
J	Moment of inertia, Kg.m^2
$\overline{m}$	Dimensionless conversion functions
MPPT	Maximum power point tracking
P	Dimensionless number of pole pairs
P_{load}	Load power, W
PMSG	Permanent magnet synchronous generator
P_{ref}	Power reference, W
PWM	Pulse width modulation
R	Load resistance, Ohm
R_s	Stator resistance, Ohm
R_t	Rotor radius of the turbine, m
S_{ic}	Dimensionless connection function
T_{em}	Generator electromagnetic torque, Nm
T_{em-ref}	Electromagnetic reference torque, Nm
T_f	Friction resistance torque, Nm
T_m	Turbine shaft torque, Nm
u_{dq-w}	Direct and quadrature adjustment voltages, V
v	Wind sped, m.s^{-1}
V_{DC}	DC bus voltage, V
v_{d-q}	d-q axis statoric voltages, V
WECS	Wind energy conversion system
Ψ_f	Permanent magnet flux, Wb
ρ	Air density, Kg.m^{-3}
λ	Dimensionless tip-speed ratio
ω	Electrical rotating speed, rad.s^{-1}
Ω	Rotor speed, rad.s^{-1}
β	Pitch angle,

Disclosures

Free Access to this article is sponsored by SARL ALPHA CRISTO INDUSTRIAL.

References

Abdulelah, A. M., Ouahid, B., & Youcef, S. Control of a stand-alone variable speed wind turbine with a permanent magnet synchronous generator. In IEEE 18th International multi-conference on systems, Signals and devices, 2021, pp. 546-550).

Agrebi, H.Z., et al. Integrated optimal design of permanent magnet synchronous generator for smart wind turbine using genetic algorithm. Energies, 2021, 14(15), p.4642.

Aissou, R., Rekioua, T., Rekioua, D., Tounzi, A. Application of nonlinear predictive control for charging the battery using wind energy with permanent magnet synchronous generator. International journal of hydrogen energy, 2016, 41(45), p. 20964-20973.

Benlahbib, Boualam, et al. Fractional order PID controller for DC link voltage regulation in hybrid system including wind turbine-and battery packs-experimental validation. International Journal of Power Electronics, 2019, 10(3), p. 289-313.

Elmorshedy, Mahmoud F., et al. Improved Standalone PMSG based wind-generating system using MPPT and MRAS for speed estimation. IEEE 4th International conference on computing, power and communication technologies (GUCON). 2021, p. 1-6.

Hostettler, J., Wang, X. Sliding mode control of a permanent magnet synchronous generator for variable speed wind energy conversion systems. Systems Science & Control Engineering, 2015, 3(1), p. 453-459.

Lee, H.J., Jin, S.K., Jae, C.K. Parameter estimation of chopper resistor in medium-voltage-direct-current during grid fault ride through. Energies, 2018, 11(12), p. 3480.

Mayouf, M., Bakhti, H., Dahmani, A. Senseless control system design of a small size vertical axis wind turbine, Jordan journal of mechanical and industrial engineering JJMIE, 2018, 12(2), p. 93-98.

Mayouf, M., Bakhti, H. Monitoring and control of a permanent magnet synchronous generator-based wind turbine applied to battery charging. Energy Sources, Part A: Recovery, Utilization, and Environmental Effects, 2021, 43(18), p. 2281-2296.

Minh, H.Q., et al. Fuzzy control of variable speed wind turbine using permanent magnet synchronous machine for stand-alone system. Sustainability in energy and buildings. Springer, Berlin, Heidelberg, 2012, p. 31-44.

Pannell, G., et al. Evaluation of the performance of a DC-link brake chopper as a DFIG low-voltage fault-ride-through device." IEEE Transactions on Energy Conversion, 2013, 28(3), p. 535-542.

Shi, K.L., Li, H. A novel control of a small wind turbine driven generator based on neural networks. In IEEE Power Engineering Society General Meeting, IEEE, 2004, p. 1999-2005.

Zhou, Xuesong, et al. DC bus voltage control of grid-side converter in permanent magnet synchronous generator based on improved second-order linear active disturbance rejection control. Energies, 2020, 13(18) p.4592.